

Human hair: subtle change in the thioester groups dynamics observed by combining neutron scattering, X-ray diffraction and thermal analysis

C.R.R.C. Lima^{1,a}, R.J.S. Lima^{2,3}, L.D.B. Machado⁴, M.V.R. Velasco⁵,
L. Lakić³, M.S. Nordentoft³, L. Machuca-Beier³, S. Rudić⁶, M.T.F. Telling^{6,7},
V. García Sakai⁶, C.L.P. Oliveira¹, and H.N. Bordallo^{3,8}

¹ Institute of Physics, University of São Paulo, São Paulo 05508-090, SP, Brazil

² Academic Unit of Physics, Federal University of Campina Grande, Campina Grande, 58429-900, PB, Brazil

³ Niels Bohr Institute, University of Copenhagen, 2300 Copenhagen, Denmark

⁴ Radiation Technology Center, Nuclear and Energy Research Institute, São Paulo, 05508-000 SP, Brazil

⁵ Faculty of Pharmaceutical Sciences, University of São Paulo, São Paulo 05508-000 SP, Brazil

⁶ ISIS Facility, Rutherford Appleton Laboratory, Chilton, Oxfordshire OX11 0QX, UK

⁷ Department of Materials, University of Oxford, Parks Road, Oxford, UK

⁸ European Spallation Source ESS ERIC, P.O. Box 176, 221 00 Lund, Sweden

Received 3 October 2019 / Accepted 29 July 2020

Published online 16 November 2020

Abstract. Hair analysis plays an important role in forensic toxicology and biomonitoring tests. However, cosmetic treatments cause changes to the hair. Thus, a better understanding of the hair's structure and the factors that influence its composition is critical. It is known that oxidative treatments modify the hair chemical, structural and mechanical properties. These treatments also cause degradation of the melanin as well as of the structures present in the hair cuticle and cortex. Considering that the literature is unanimous regarding the increase in hydrophilicity and porosity promoted in human hair by bleaching, in this work we investigated how this oxidative damage is triggered. By combining several techniques, inelastic and quasi-elastic neutron scattering, differential scanning calorimetry, thermal gravimetric analysis and X-ray diffraction, we were able to connect the chemical and structural changes to a subtle dynamic modification of the proton mobility in the hair fibers. In addition, alterations in the thermal behavior evidenced a small denaturation of α -keratin intermediate filaments and a slight decrease in the amount of confined water in the hair fibers. Moreover, data obtained by neutron spectroscopy indicated that bleaching attacks the thioester groups of the proteins causing larger proton mobility of the hydrogenous components (water, protein and/or lipids).

^a e-mail: cibelelima@usp.br

1 Introduction

Human hair is a biopolymer showing two major distinct morphological regions: the cuticle (with a total thickness of roughly $0.5\ \mu\text{m}$) and the cortex (formed by spindle-shaped cells with $0.1\text{--}0.4\ \mu\text{m}$ in width) [1]. The cortex contains a helical fraction that comprises a crystalline phase (α -keratin intermediate filaments – IFs) embedded in an amorphous matrix of IF-associated proteins (IFAPs) [2]. The main function of the cuticle, the outer structure of mature hair, is to provide mechanical protection for the cortex. These chemical structures within hair create unique physical characteristics, where the strong disulfide bonds linking adjacent keratin chains produce a fibrous structure significantly resistant to chemical and biological degradation [1,3]. Even if the hair fibers possess quite complex composition and morphology, which are also relatively distinct from one individual to another, the following main components are often considered: fibrous proteins (mostly keratins, 85–93%), melanin (complex polymers derived from tyrosine responsible for the hair natural color), water (3–15% by mass), lipids (1–9%) and mineral compounds (0.25–0.95%). The bulk of the volume within a cortical cell is comprised of long cystine-containing macrofibrils, each with a diameter between 40 and 200 nm [4]. It is well known that cosmetic treatments, like bleaching, straightening and/or dyeing, cause changes in the hair structure, including the IFs [3,5] and other microstructures of the amorphous matrix [1,6,7]. In the particular case of chemical bleaching, destruction of the chromophoric groups of hair pigments in the cortex along with side reactions with the hair proteins, takes place. This process can be understood as follows. The oxidizing agent (normally hydrogen peroxide) which has pHs between 9 and 11 attacks the thioester groups that bind 18-methyl eicosanoic acid to the surface proteins, creating sulfonate groups on the fiber surface, which in turn results in an acidic, hydrophilic hair surface with a lower isoelectric point [1,3]. These effects lead to the oxidation and cleavage of cystine groups, predominately occurring via a S–S fission route [1,3,5], which results in changes to the hair's properties.

Up to date a variety of techniques have been used to evaluate the oxidative damage in the hair structure [3,5,8–11]. In this work we used neutron scattering, a technique rare to this area of science, to investigate the effects of oxidative chemistry on human hair. Neutron spectroscopy is an ideal tool to study the structure and dynamics of confined water and proteins and the strength of the H-bond interactions can be straightforwardly obtained [12,13]. In this context, we combined inelastic and quasi-elastic neutron scattering (INS and QENS) with small angle X-ray scattering (SAXS) and thermal analysis (thermogravimetry – TGA – and differential scanning calorimetry – DSC). Our main goal is to determine possible changes in the α -keratin IFs and the matrix of the hair as well as on how the hydrogen mobility is affected by chemical treatments, i.e. bleaching.

2 Experimental details

2.1 Sample preparation

Caucasian dark brown hair samples, untreated and in the form of tresses (2 g and 10 cm long) were purchased from DeMeo Brothers® (New York). After being washed with a 10% w/w dispersion of sodium ether lauryl sulfate and dried at room temperature, the selected hair tresses were bleach damaged using a commercial treatment product based on an alkaline solution (pH 10.5) in the oxidant medium of hydrogen

peroxide (20 vol) and ammonium persulfate, applied for 30 min and at room temperature. This treatment was followed by rinsing and air-drying. The remaining samples were kept intact, i.e. virgin hair.

2.2 Thermal analysis (TGA and DSC)

TGA measurements were performed on a TGA 209 F1 (Netzsch), on hair snippets inserted in an open Al_2O_3 crucible containing 5–10 mg of sample using a heating rate of 10 K/min. To assure reproducibility, two types of measurements, hereafter named procedure (i) and (ii) were performed. During procedure (i), TGA curves were obtained with continuous heating between 30 and 400 °C under N_2 atmosphere (50 mL/min) on batch of snippets stored under standard room conditions (25 °C, 30% relative humidity (RH)), while for procedure (ii), analogously to [14] and [15], the samples were prepared at RH of 58% using a saturated solution consisting of 50 mL of demineralized water and 100 g natrium-bromide (NaBr), heated to 180 °C and kept at this temperature (isotherm phase) for 15 min. Afterwards, the samples were continuously heated to 450 °C. This procedure ensures that the mass change due to water loss is separated from the loss caused by sample degradation. To prepare the samples at 58% RH, the saturated solution was first poured into a desiccator, where a metal mesh was used to separate the liquid from the samples, and subsequently, to allow the samples to hydrate homogenously, the hair snippets were carefully placed in small pierced plastic containers. The desiccator was then cautiously sealed to create an isolated atmosphere and the samples were left hydrating for at least 24 hours prior to the measurements. A protective N_2 gas flow of 20 mL/min was used during (ii) and the data were collected in triplicate.

DSC measurements, performed in triplicate on both hair samples immersed in water, were conducted on a power-compensated instrument (DSC 6000, Perkin-Elmer, USA), using stainless steel, large volume pans, which are pressure resistant up to 25 bar. The temperature range was 50–180 °C with a heating rate of 10 K/min [3]. Hair snippets (~5 mg) were weighed into the DSC-pans and 40 μL of water added. The pans were sealed and stored overnight prior to the DSC-measurement.

2.3 Small-Angle X-ray scattering (SAXS)

SAXS data were collected in a transmission geometry on hair tresses joined and oriented in the vertical direction inside the sample holder. The measurements were performed on a Xeuss 2.0 from Xenocs, with Cu $K\alpha$ radiation, $\lambda = 1.54 \text{ \AA}$. 2D scattering intensities were collected on an Pilatus 300k detector with sample to detector distance equal to 0.98 m, which provided a momentum transfer modulus of $0.0125 \text{ \AA}^{-1} < q < 0.17 \text{ \AA}^{-1}$, where q is defined as $q = 4\pi \sin(\theta)/\lambda$ and 2θ is the scattering angle. Since one has anisotropic scattering, due to the alignment of the hair tresses, it was necessary to perform angular cuts on the images, see Figure 1. For this we used the Fit2D program [16], which allowed to integrate different areas of the 2D diffractograms (SAXS and WAXS) and thus obtain one dimensional scattering intensity graphs, Figure 3, as a function of the scattering vector module (q).

2.4 Neutron spectroscopy

Hydrogen mobility in both samples was investigated using quasi-elastic neutron scattering (QENS) by means of the elastic fixed window (EFW) method [17]. Using this

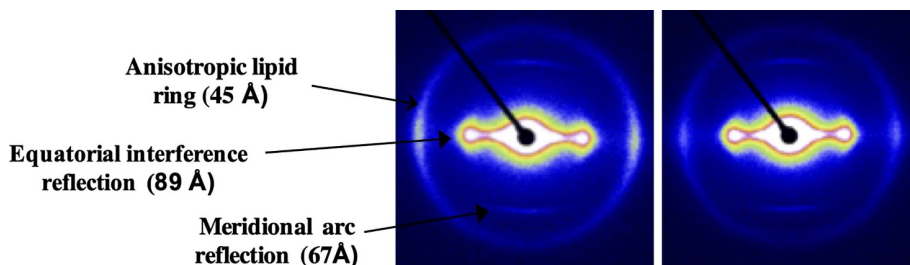


Fig. 1. Typical 2D SAXS scattering intensity for a virgin hair sample (a) and for a bleached hair sample (b). It is interesting to observe the differences in the latter hallow. The resulting SAXS diffractograms are shown in Figure 2b.

methodology, we assess the evolution of only those neutrons scattered elastically by the sample as a function of temperature. Analysis of elastic scattering response allows determining the onset of proton mobility by noting points of inflexion in the data. The mobility of the hydrogen in the hair matrix was measured between 10 and 300 K with data collected upon heating. The data, collected at the backscattering spectrometer IRIS [18], located at the ISIS Facility in the UK, provides an elastic energy resolution of $17.5 \mu\text{eV}$ at full width at half maximum (FWHM), corresponding to an upper experimental observation time of ~ 200 ps, was normalized to the response observed at the lowest temperature. Information on molecular vibrations occurring over a broad energy range from 1 to 1000 meV, corresponding to the femtosecond, fs, domain, was obtained using indirect geometry time-of-flight neutron spectrometer TOSCA [19], also located at ISIS. INS spectra for all samples were recorded at 10 K. During these experiments the samples were confined in flat plate aluminum containers sealed with Indium wire. The collected data were converted to the incoherent dynamic structure factor, $S(Q, \omega)$, using the Mantid software [20]. The data were normalized to sample mass and subsequently to the intensity of the elastic line.

3 Results and discussion

Figure 2a shows the TGA curves obtained according to procedures (i) and (ii), (described in Sect. 2.2). Figure 2a shows the data collected with continuous heating, where two mass loss events are observed: the first relates to water release from 30 up to 180°C and the second to the denaturation of the hair keratin, with degradation of proteins and components of the amorphous matrix, between 200 and 400°C . The reproducibility of the hair dehydration process was verified by the experiments realized in triplicate according to (ii). Table 1 gives the approximate moisture content (water loss in %) using both procedures. The effect of RH on the water content of virgin human hair is in full agreement with the literature [1]. Furthermore, the evaluation of water loss from both sets of data confirms previous observations showing that bleaching leads to liquid retention [1,15,21–25]. On further heating, i.e. above 180°C , and independently of measurement approach, it was observed that the bleached hair showed a lower mass loss when compared to the virgin sample. These results substantiate previous findings, where it was considered that in the process of bleaching the hair loses mass (proteins and lipids) [1,21–23]. In addition, the oxidative treatment causes hydrolysis of the amide groups of the amino acids plus formation of cysteic acid residues, resulting in an increase of the acidic groups in the fibers followed by a decrease of their isoelectric and isoionic points [1,23,26].

Figure 2b shows the DSC curves for virgin and bleached hair, acquired in triplicate (see Tab. 1 as well). From these data a tiny decrease of the α -helical proteins'

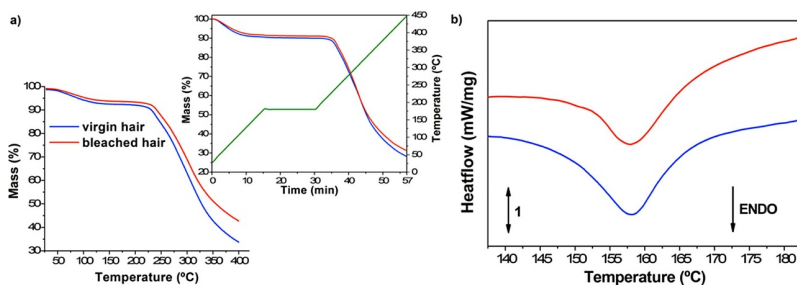


Fig. 2. Averaged (a) TGA and (b) Representative DSC curves of the virgin (blue) and bleached (red) hair. The top figure in (a) shows the data obtained using procedure (ii).

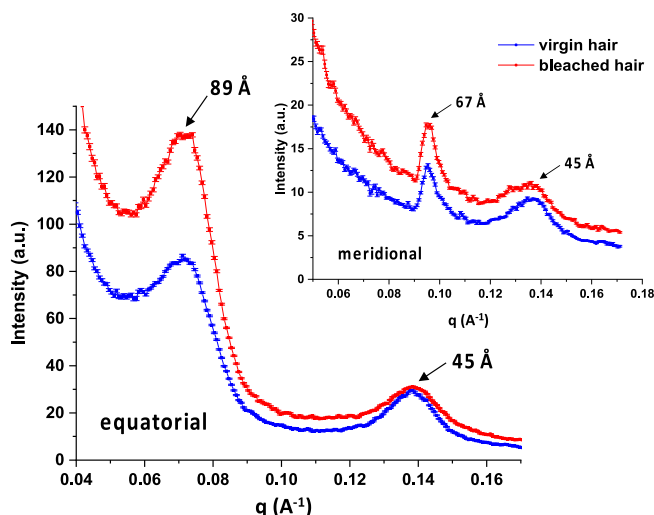


Fig. 3. SAXS diffractograms of the virgin and bleached hair tresses.

denaturation enthalpy (ΔH_D) in the intermediate filaments and an increase in the protein denaturation temperature, T_D , are observed. Such increase of the denaturation peak maximum temperature (T_D) has been previously observed in samples where the oxidative treatment was reapplied [22]. These effects can be related to the loss of crystalline material (α -keratin IFs) promoting the weakening of the fiber, and consequent alteration of their properties [3,21,22].

This idea also corroborates with the SAXS data (Fig. 3), in which the bleached hair shows alterations in the intensity of the equatorial reflections located at about 45 and 89 Å. Kreplak et al. [25] described this phenomenon as a change of the distance between IFs (crystalline organization).

In addition to the thermal induced changes, it has been recently reported that S-S bond reduction treatments (such as bleaching) affect the hair structure and water permeability [13]. Moreover, it has been also argued that bleaching disturbs the disulfide bonds, causing the conversion of cystine disulphide bonds to cysteic acid, while cortical proteins convert to a random coil structure [27]. Thus, to evaluate how and if oxidative damage promotes alterations in the hydrogen mobility within the hair fiber we used neutron spectroscopy. EFW results (Fig. 4a), represented as mean square displacements (MSD) [28], obtained for the averaged Q-values, show that for bleached hair, the hydrogen atoms are slightly freer to move when compared to the virgin hair, indicating that the structure of the bleached hair is somehow more flexible

Table 1. Results of mass loss of dehydration (TGA): for procedure (i) the mass loss was taken at 180 °C, while for procedure (ii) the approximate moisture content taken after the isotherm phase, i.e. after 15 minutes of data collection, using the mean value*; helical fraction denaturation (ΔH_D) and denaturation peak temperature (T_D) of hair samples.

Events	Virgin hair		Bleached hair	
	Procedure (i)	Procedure (ii)	Procedure (i)	Procedure (ii)
Approximate moisture content/TGA%	6.6	10.0 ± 0.06	5.7	8.91 ± 0.08
Denaturation/DSC	$T_D/^\circ\text{C}$	155.1 ± 1.5	157.6 ± 0.7	
	$\Delta H_D/\text{J/g}$	17.5 ± 0.9	15.0 ± 0.9	

*(ii): Based on [1] one sample from each triplicate was an outlier and therefore not used in the calculations of moisture content (%).

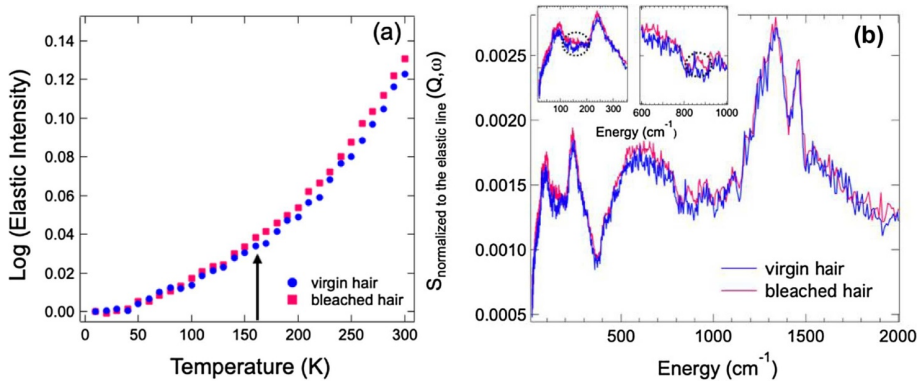


Fig. 4. (a) Normalized evolution of immobile protons on the ns-time scale obtained from data collected using IRIS at ISIS. The error bars are within the size of the symbols. (b) Normalized vibrational spectra obtained at 10 K using the vibrational spectrometer TOSCA. Virgin hair samples are shown in blue and bleached samples are shown in red. In (a) the anomalous decrease of the elastic intensity, indicated by arrow and occurring around 160 K, is indicative of the onset of some type of diffusive motion that is faster than the instrumental time resolution (200 ps). In (b) the intensity of the signal is directly proportional to the phonon density.

when compared to the virgin hair, making it more susceptible to intermediate chemical reactions due to the sulfur acids from the oxidative process. This also explains the larger intensity of the INS spectra for the bleached hair when compared to the virgin sample (Fig. 4b). Furthermore, we are able to identify small changes in the vibrational modes assigned to the hydrogen atoms around 150 cm^{-1} and 950 cm^{-1} (detail in Fig. 4b). Considering that these particular vibrations, which are extremely difficult to observe using infrared or Raman spectroscopy, are assigned to S–H torsion and S–H bending in L-cysteine [28,29], we can argue that these changes to the sulfhydryl (–SH) group vibrations experimentally confirm that chemical bleaching attacks the thioester groups present in the cuticle and in the cystine amino acids forming the cuticle and the cortex. This modification makes the structure less rigid and in turn the proton mobility increases. It is known that the thiol (–SH) group of cysteine is highly reactive and will readily oxidize to covalently bind with another cysteine residue to form a disulfide bond (–S–S–), forming cystine. Such bonds are a major contributor to the rigidity and mechanical properties [1,14].

In this work, we related a single bleaching application to the development of the changes in IFs and amorphous matrix by neutron spectroscopy, X-ray scattering and

thermal analysis. It was shown that this analytical approach enables the detection of specific regions of damage within hair fiber. It is noteworthy to point out that inelastic neutron scattering ought to be considered an ideal analytical method to get insight on the partial oxidation products of cystine and the formation of the cysteic acid in treated human hair. Furthermore, the results obtained with INS are particularly interesting since it is very difficult to measure traces of cysteine [30], implying that this approach can be extended to other biological studies.

C.R.R.C.L, L.D.B. M, M.V.R.V. and C.L.P. O. acknowledge financial support of this work by CAPES, the National Institute of Science and Technology Complex Fluids (INCT-FCx), Conselho Nacional de Desenvolvimento Científico e Tecnológico (CNPq) and Fundação de Amparo à Pesquisa do Estado de São Paulo (FAPESP)/São Paulo/Brazil. RJSL acknowledges financial support from UFCG for a research visit at the NBI. RJSL and HNB also acknowledge the support for neutron and X-ray research given by Danscatt the Danish Agency for Science, Technology and Innovation. All authors thank the Science and Technology Facilities Council (STFC) for access to neutron beamtime at the ISIS Facility (RB1810591 and XB1890151).

Publisher's Note The EPJ Publishers remain neutral with regard to jurisdictional claims in published maps and institutional affiliations.

References

1. C.R. Robbins, *Chemical and physical behavior of human hair* (Springer-Verlag, New York, 2012)
2. M. Feughelman, *Text. Res. J.* **29**, 223 (1959)
3. F.-J. Wortmann, C. Springob, G. Sendelbach, *J. Cosmet. Sci.* **53**, 219 (2002)
4. I.M. Kempson, E. Lombi, *Chem. Soc. Rev.* **40**, 3915 (2011)
5. D. Istrate, C. Popescu, M. Er Rafik, M. Möller, *Polym. Degrad. Stab.* **98**, 542 (2013)
6. L. Coderch, S. Méndez, M. Martí, R. Pons, J.L. Parra, *Colloids Surf. B.* **60**, 89 (2007)
7. M. Baias, D.E. Demco, C. Popescu, R. Fechete, C. Melian, B. Bluemich, M. Moller, *J. Phys. Chem. B*, **113**, 218 (2009)
8. L. Kreplak, J. Doucet, P. Dumas, F. Briki, *Biophys. J.* **87**, 1 (2004)
9. C.R.R.C. Lima, M.M. Almeida, M.V.R. Velasco, J.R. Matos. *J. Therm. Anal. Calorim.* **123**, 2321 (2015)
10. C.R.R.C. Lima, R.A.A. Couto, T.B. Freire, A.M. Goshiyama, A.R. Baby, M.V.R. Velasco, V.R.L. Constantino, J.R. Matos, *J. Cosmet. Dermatol.* **18**, 1885 (2019)
11. V. Stanic, J. Bettini, F.E. Montoro, A. Stein, K. Evans-Lutterod., *Sci. Rep.* **5**, 17347 (2015)
12. Y. Kamath, N.S. Murthy, R. Ramaprasad. *J. Cosmet. Sci.* **65**, 37 (2014)
13. N.S. Murthy, W. Wang, Y. Kamath, *J. Struct. Biol.* **206**, 295 (2019)
14. F.J. Wortmann, G. Wortmann, J. Marsh, K. Meinert, *J. Struct. Biol.* **177**, 553 (2012)
15. C. Barba, S. Méndez, M. Martí, J.L. Parra, L. Coderch, *Thermochim. Acta* **494**, 136 (2009)
16. A.P. Hammersley, *J. Appl. Crystallogr.* **49**, 646 (2016)
17. A.K. Lauritsen, J.E.M. Pereira, F. Juranyi, H.N. Bordallo, L. Larsen, A.R. Benetti, *J. Dent. Res.* **97**, 1017 (2018)
18. S.I. Campbell, M.T.F. Telling, C.J. Carlile, *Physica B* **276-278**, 206 (2000)
19. R.S. Pinna et al., *Nucl. Instrum. Methods Phys. Res. A* **896**, 68 (2018)
20. O. Arnold et al., *Nucl. Instrum. Methods Phys. Res. A* **764**, 156 (2014)
21. A.J. Grosvenor, S. Deb-Choudhury, P.G. Middlewood, A. Thomas, E. Lee, J.A. Vernon, J.L. Woods, C. Taylor, F.I. Bell, S. Clerens, *Int. J. Cosmet. Sci.* **40**, 536 (2018)
22. V.F. Monteiro, A.P. Maciel, E. Longo. *J. Therm. Anal. Calorim.* **79**, 289 (2005)
23. M.N. Chandrashekhara, C. Ranganathaiah, *J. Photochem. Photobiol. B* **101**, 286 (2010)

24. S.B. Ruetsch, Y.K. Kamath, in *IFSCC Magazine* (2005), p. 142
25. L. Kreplak, A. Franbourg, F. Briki, F. Leroy, D. Dallé, J. Doucet, *Biophys. J.* **82**, 2265 (2002)
26. B.C. Beard, A. Johnson, F.M. Cambria, P.N. Trinh. *J. Cosmet. Sci.* **56**, 65 (2005)
27. A. Kuzuhara, *Biopolym.* **81**, 506 (2006)
28. H.N. Bordallo, E.V. Boldyreva, J. Fischer, M.M. Koza, T. Seydel, V.S. Minkov, V.A. Drebuschak, A. Kyriakopoulos, *Biophys. Chem.* **148**, 34 (2010)
29. A. Pawlukojs, J. Leciejewicz, A.J. Ramirez-Cuesta, J. Nowicka-Scheibe, *Spectrochim. Acta Part A* **61**, 2474 (2005)
30. T. Ishii, G.E. Mann, *Redox Biol.* **2**, 786 (2014)